Biochemical and Biophysical Research Communications 421 (2012) 721–726

Contents lists available at SciVerse ScienceDirect

Biochemical and Biophysical Research Communications

journal homepage: www.elsevier.com/locate/ybbrc

Tellurite-exposed *Escherichia coli* exhibits increased intracellular α-ketoglutarate

Claudia A. Reinoso [a], Christopher Auger [b], Vasu D. Appanna [b], Claudio C. Vásquez [a,*]

[a] Departamento de Biología, Facultad de Química y Biología, Universidad de Santiago de Chile, Santiago, Chile
[b] Department of Chemistry and Biochemistry, Laurentian University, Sudbury, Ontario, Canada

ARTICLE INFO

Article history:
Received 12 April 2012
Available online 20 April 2012

Keywords:
Tellurite
α-Ketoglutarate
Superoxide
Reactive oxygen species
Oxidative stress

ABSTRACT

The tellurium oxyanion tellurite is toxic to most organisms because of its ability to generate oxidative stress. However, the detailed mechanism(s) how this toxicant interferes with cellular processes have yet to be fully understood. As part of our effort to decipher the molecular interactions of tellurite with living systems, we have evaluated the global metabolism of α-ketoglutarate a known antioxidant in *Escherichia coli.* Tellurite-exposed cells displayed reduced activity of the KG dehydrogenase complex (KGDHc), resulting in increased intracellular KG content. This complex's reduced activity seems to be due to decreased transcription in the stressed cells of *sucA*, a gene that encodes the E1 component of KGDHc. Furthermore, it was demonstrated that the increase in total reactive oxygen species and superoxide observed upon tellurite exposure was more evident in wild type cells than in *E. coli* with impaired KGDHc activity. These results indicate that KG may be playing a pivotal role in combating tellurite-mediated oxidative damage.

1. Introduction

Tellurium is a metalloid belonging to the VIA group of the periodic table of elements that shares various chemical properties with biologically important elements such as oxygen, sulfur, and selenium [1]. Although in its elemental form, Te°, tellurium is rather scarce in nature, the soluble oxyanions tellurite (TeO_3^{-2}) and tellurate (TeO_4^{-2}) are highly toxic to both prokaryotic and eukaryotic cells [2]. Experimental evidence accumulated during the last few years suggests that tellurite toxicity is due, at least in part, to the generation of reactive oxygen species (ROS) [3–6]. Tellurite-mediated ROS generation was first suggested in studies showing that tellurite minimal inhibitory concentrations (MIC) were higher for tellurite-hypersensitive *Escherichia coli sodAsodB* under anaerobic conditions [7]. The leading ROS generated as consequence of tellurite exposure was shown to be superoxide (O_2^-) [4]. In fact, it was later shown that this radical, produced concomitantly with tellurite reduction, was responsible for the abolition of fumarase and aconitase activity in tellurite-exposed *E. coli* [8].

On the other hand, studies using extracts from *Aeromonas caviae* ST and *E. coli* previously grown in the presence of increasing K_2TeO_3 concentrations showed that while pyruvate dehydrogenase (PDH) activity decreased by ~40%, tellurite reductase (TR) activity increased almost 2-fold. Only dihydrolipoamide dehydrogenase (E3 component of PDH) was shown to display TR activity *in vitro* [9]. Because E3 also forms part of the α-ketoglutarate dehydrogenase complex (KGDHc) [10] tellurite might also affect the normal functioning of this complex, thus representing another intracellular target of the toxicant [9]. In this context, a perturbation of various key TCA cycle enzymes activity leading to α-ketoglutarate (KG) accumulation has been observed in *Pseudomonas fluorescens* and eukaryotic HepG2 cells exposed to ROS-generating compounds [11].

KG, an intermediary α-keto acid of the TCA cycle, can detoxify H_2O_2 and O_2^- through spontaneous decarboxylation to yield succinate [12]. It has been proposed that by decreasing KGDHc and increasing isocitrate dehydrogenase (ICDH) activities, cells seem to dedicate some KG to ROS-scavenging with the concomitant drop in NADH biogenesis. Thus, reducing KGDHc activity seems to be pivotal in TCA cycle regulation [11]. In this context, KGDHc activity modulation could play a key role in the cell's ROS-detoxifying strategy.

In this work, we evaluated KG's participation in facing tellurite-induced oxidative stress in *E. coli*. KGDHc activity and KG content was examined in tellurite-exposed *E. coli*. Tellurite sensitivity and ROS content was assessed in wild type and *E. coli* cells lacking *sucA*, *sucB* or *lpdA*, encoding E1 (ketoglutarate dehydrogenase), E2 (dihydrolipoyl transacetylase) and E3 (dihydrolipoyl dehydrogenase) KGDHc components, respectively. Results showed decreased KGDHc activity and increased KG content in toxicant-treated bacteria, suggesting that KG accumulation may represent a strategy to cope with tellurite-mediated oxidative damage in *E. coli*. Reduced KGDHc activity seems to result from decreased *sucA*

---

* Corresponding author. Address: Laboratorio de Microbiología Molecular, Departamento de Biología, Facultad de Química y Biología, Universidad de Santiago de Chile, Casilla 40, Correo 33, Santiago, Chile. Fax: +56 (2) 681 2108.

E-mail address: claudio.vasquez@usach.cl (C.C. Vásquez).

0006-291X/$ - see front matter © 2012 Elsevier Inc. All rights reserved.
http://dx.doi.org/10.1016/j.bbrc.2012.04.069

transcription in stressed cells. Finally, it was observed that *E. coli* exhibiting impaired KGDHc activity generates less ROS than the wild type strain.

2. Materials and methods

2.1. Bacteria and growth conditions

Bacterial strains used in this work are listed in Table 1. Cells were routinely grown in Luria–Bertani (LB) medium at 37 °C with shaking. Growth was started by inoculating 1:100 dilutions of overnight cultures in fresh medium. When required, kanamycin (100 μg/ml) was amended to the medium.

2.2. Growth inhibition zone (GIZ) and minimal inhibitory concentration (MIC) determination

GIZ were determined as described earlier [13]. In brief, cultures were grown to OD_{600} $\sim$0.5 and 100 μl aliquots were evenly spread on LB-agar plates. After air drying, 10 μl of K_2TeO_3 10,000 μg/ml were deposited on sterile filter disks (6 mm) previously placed on the plate centers. Growth inhibition zones were determined after overnight incubation at 37 °C.

MICs were assessed as follows. Sterile stock solutions of appropriate K_2TeO_3 concentrations were serially diluted in 96-well ELISA plates containing 200 μl of LB medium amended with the appropriate antibiotic per well. Cultures (5 μl) grown to OD_{600} $\sim$0.5 were added to each well and plates were incubated at 37 °C. Turbidity was observed visually after 24 h.

2.3. Assessment of intracellular KG and succinate content

KG levels were determined by high-performance liquid chromatography (HPLC). Cells *E. coli* BW25113 (wild type) were grown in LB medium and exposed to 0.5 μg/ml tellurite for 5, 15 or 30 min. After centrifuging at 8000*g* for 3 min, cells were washed and suspended in 350 μl of 25 mM phosphate buffer pH 7.0. After sonication, the cell debris was discarded and supernatants were treated with 200 μl of 0.5% (v/v) perchloric acid and centrifuged and filtered before injection into an Alliance HPLC (Waters) apparatus equipped with an Agilent Hi-Plex H (300 × 7.7 mm) column operating at a flow rate of 0.6 ml/min. Runs lasted 30 min. KG and succinate were detected at 210 nm using a dual wavelength absorbance detector. The mobile phase was 5 mM H_2SO_4 at 55 °C. Metabolites were identified by comparison with known standards and bands were quantified using the Empower software (Waters Corporation). Protein concentration was normalized as described earlier [14].

2.4. qRT-PCR

Cells grown in LB medium to OD_{600} $\sim$0.5 were exposed to 0.5 μg/ml tellurite for 30 min. Total RNA was purified using the RNAsy kit (Qiagen), as recommended. Two micrograms of purified RNA was used as template for qRT-PCR. Reactions were performed using the LightCycler RNA Amplification SYBR Green I kit (Roche Applied Science) as recommended by the vendor. Transcript amounts (ng) of *sucA, sucB and lpdA* mRNA were calculated from a standard curve made with known template concentrations. Specific primers used to amplify the genes under study are indicated in Table 1. *rpoD* was used to normalize the experiment.

2.5. ROS monitoring by flow cytometry

To determine total ROS, *E. coli* BW25113 and KGDHc mutants were grown to OD_{600} $\sim$0.5 and exposed to 0.05 μg/ml tellurite for 30 min. After washing, centrifuging and suspending in 500 μl of 25 mM phosphate buffer pH 7.0 (buffer A), cells were incubated with 0.02 mM 2,7 dihydrodichlorofluorescein diacetate (H_2CFDA, final concentration) for 30 min in the dark. Fluorescence intensity was monitored as above (λ_{ex} 428, λ_{em} 522). Data acquisition was performed by counting the number of positive cells as recently described [15]. Cells exposed to 5 mM TBH (tert-butyl hydroperoxide) were used as positive control for total ROS detection.

To assess superoxide, *E. coli* BW25113 and KGDHc mutants strains were grown to OD_{600} $\sim$0.5 and exposed to 0.05 μg/ml tellurite for 30 min. After centrifuging and washing with buffer A, cells were suspended in 500 μl of buffer A and incubated with 0.05 mM dihydroethidine (DHE, final concentration) for 15 min in the dark. Intensity was assessed using a Becton Dickinson (model FacsCanto II) apparatus equipped with an Argon laser (λ_{ex} 520, λ_{em} 610). Tellurite-exposed Δ*sodAsodB E. coli* was used as tool for oxidized DHE detection.

2.6. KGDHc, complex I and NADH oxidase activity determination

KGDHc activity was assayed at 37 °C in cell-free extracts from tellurite-exposed *E. coli* (0.5 μg/ml, 30 min). NAD^+ reduction was monitored at 340 nm for 1 min. The reaction mixture (1 ml) contained 25 mM Tris–HCl buffer, pH 7.0, 0.5 mM NAD^+, 10 mM KG, 20 mM $MgSO_4$, 1 mM CoASH and 4 mM TPP. Assays were started with the extract (100 μg protein) [16]. Blue native polyacrylamide gels were run for in-gel visualization of enzyme activity. Assays were started with the extract (300 μg protein) coupling NADH/NADPH formation to 0.3 mg/ml phenazine methosulfate and 0.5 mg/ml iodonitrotetrazolium as decribed [17].

Complex I and NADH oxidase activity was assessed at 37 °C in cell-free extracts from tellurite-exposed *E. coli* (0.5 μg/ml, 30 min). Blue native polyacrylamide gels were run for in-gel

Table 1
E. coli strains and primers used in this study.

Strain	Relevant genotype	Source or reference
BW25113	Δ *(araD-araB)567*, Δ*lacZ4787*(::*rrnB*-3),	[24]
Δ*sucA*	BW25113 *sucA* (*icdA*::Kan^R)	[24]
Δ*sucB*	BW25113 *sucB* (sucB::Kan^R)	[24]
Δ*lpdA*	BW25113 *lpdA* (*lpdA*::Kan^R)	[24]
Primers	Forward (F) or Reverse (R), to amplify	5′–3′ Sequence
sucA F	F, *sucA*	ATGCAGAACAGCGCTTTGAA
sucA R	R, *sucA*	CGGAAATATTCACGCGTTTG
sucB F	F, *sucB*	CTGACCTGCCTGAATCCGTA
sucB R	R, *sucB*	ACCAAGGATCTGACGAGACG
lpdA F	F, *lpdA*	GTACTGAAATCAAAACTCAGGTCG
lpdA R	R, *lpdA*	CGCTTTGGCTTCTTCGATAA

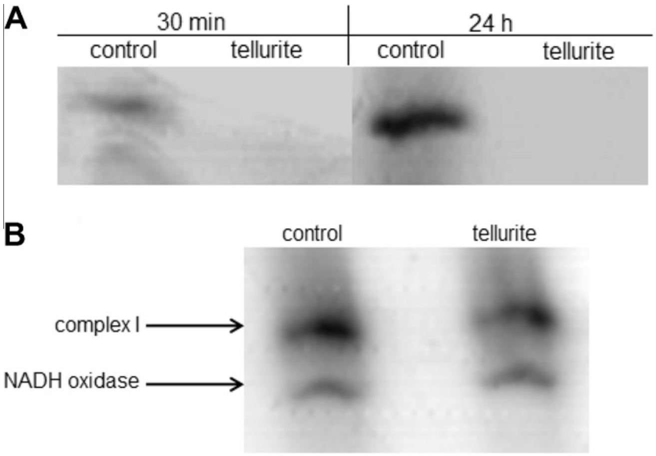

Fig. 1. *In situ* KGDHc, complex I and NADH oxidase activity. KGDHc (A) and complex I and NADH oxidase activities (B) were assayed after fractionating extracts from tellurite-treated cells by native gradient polyacrylamide gels as described in Section 2. Representative gels are shown.

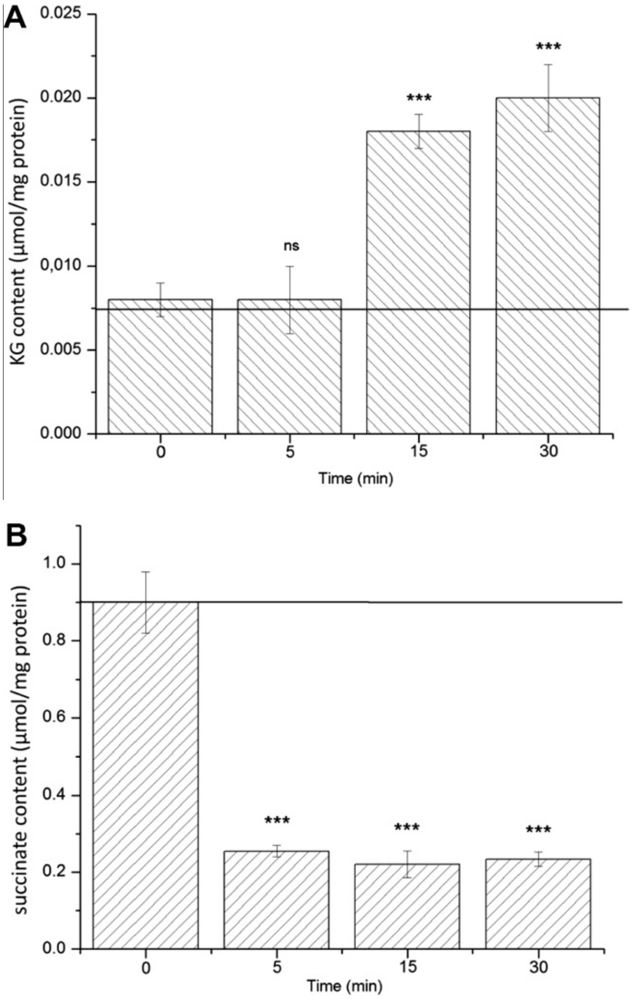

Fig. 2. Metabolite assessment in tellurite-exposed wild type *E. coli*. KG (A) and succinate (B) contents in wild type *E. coli* exposed to 0.5 µg/ml tellurite for 5, 15 and 30 min. were assessed by HPLC as described in Section 2. The line represent negative control for both compounds (no tellurite added). Numbers represent the mean of 3 independent trials. ns, non significant.

visualization of enzyme activity and then incubated with 25 mM Tris–HCl pH 7.4, 5 mM $MgCl_2$ buffer for 15 min. Assays were started with the extract (100 µg protein), after adding 5 mM NADH and 5 mM KCN, 0.4 mg/ml iodonitrotetrazolium and 0.2 mg/ml dichlorophenol indophenol were used to reveal the activity [17].

Table 2
Tellurite GIZ (cm^2) and MIC (µg/ml) for the indicated *E. coli* strains.

Strains	GIZ	MIC
BW25113	7.1	0.8
Δ*sucA*	7.4	0.4
Δ*sucB*	7.8	0.4
Δ*lpdA*	9.9	0.1

GIZs and MICs were determined in LB medium as described in Section 2. Numbers are the mean of 3 independent trials.

2.7. Data analysis

In general, results were expressed as the mean ± the standard deviation. Differences between experimental groups were analyzed using one-way ANOVA. *P* values less than 0.05 were considered statistically significant.

3. Results and discussion

3.1. *E. coli* exposure to tellurite results in decreased KGDHc activity and unchanged complex I and NADH oxidase activities

To assess the effect of tellurite on KGDHc activity, extracts from tellurite-exposed cells were used. As determined by a spectrophotometric assay, enzymatic activity decreased ~30% when wild type *E. coli* was exposed to the toxicant for 30 min (Fig. S1A). KGDHc activity was also assessed *in situ*, after fractionating crude extracts from cells exposed or not to tellurite by non-denaturing polyacrylamide gel electrophoresis. KGDHc activity was practically undetected even after 24 h exposure (Fig. 1A). KGDHc activity abolition could be the consequence of a direct effect of tellurite on enzyme activity/structure or indirect, at the transcriptional level thus affecting mRNA synthesis for one (or more) KGDH components (see below).

On the other hand, it has been proposed that KG decarboxylation -with the concomitant NADH formation- would increase the oxidative status of the cell [18]. KGDHc inhibition/inactivation would help to alleviate the effects of tellurite-mediated oxidative damage. In this context, there are other examples regarding the role that metabolic enzymes could play in controlling oxidative damage caused by certain elicitors as aluminum [19] or tellurite [8,9].

Given that limiting NADH production is crucial under oxidative stress conditions and since the activity of NADH-using enzymes usually decreases in these circumstances [20], the activity of complex I and NADH oxidase was assessed. No significant changes in these activities were observed in tellurite-exposed cells when compared with untreated controls (Fig. 1B), evidencing the importance of decreasing NADH levels through KGDHc inhibition to alleviate tellurite-mediated oxidative stress.

3.2. KG accumulates in tellurite-exposed *E. coli* cells

Since KGDHc activity decreases in tellurite-exposed *E. coli*, KG content was assessed by high performance liquid chromatography (HPLC). Higher KG levels were found in tellurite-exposed wild type cells in regard to untreated controls (Fig. 2A). These results suggest that KG may accumulate because of the decrease of KGDHc activity. Results supporting this came from the observation that decreased ICDH and GDH KG-synthesizing activities were found in

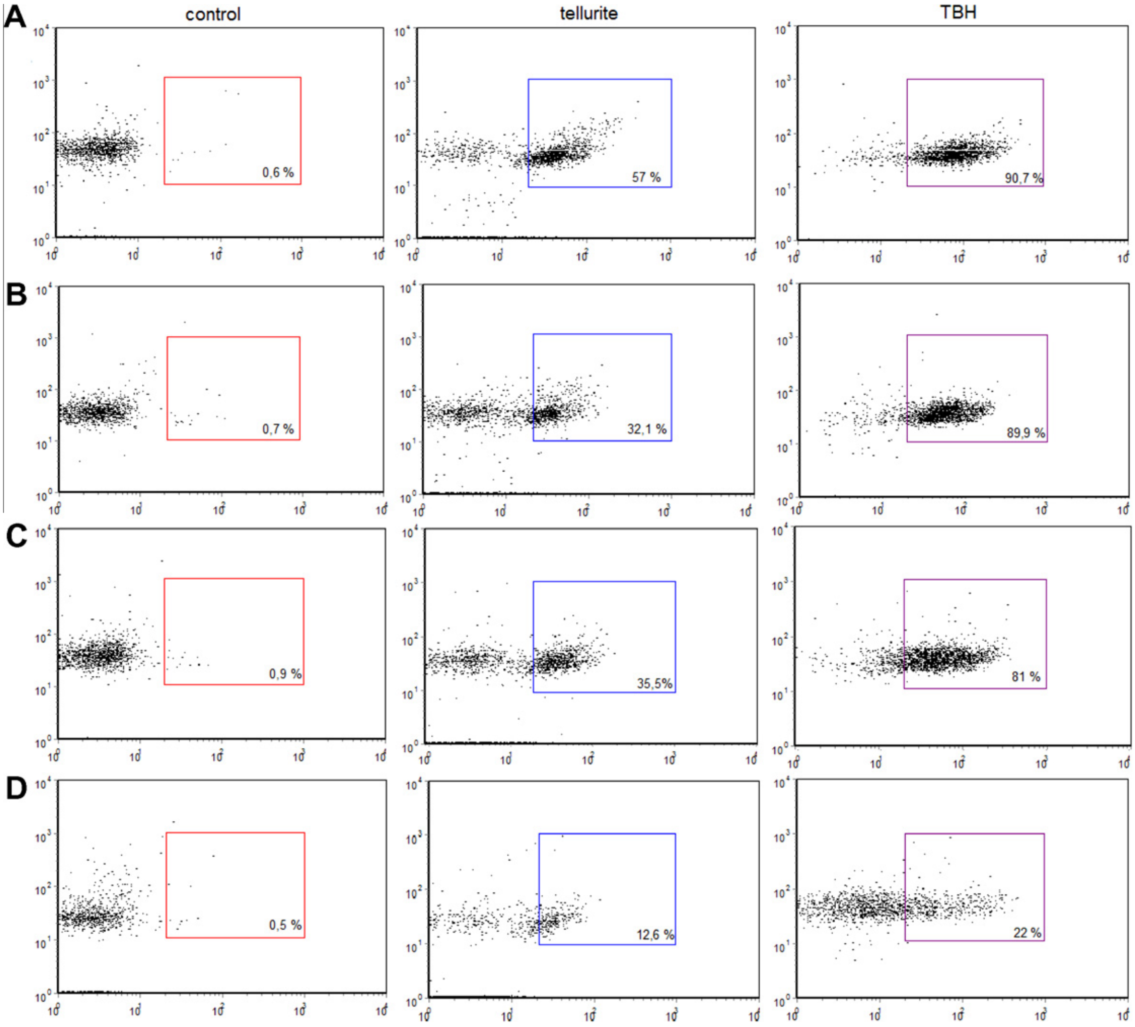

Fig. 3. Total ROS levels in tellurite-exposed *E. coli*. The indicated *E. coli* strains exposed or not to tellurite or tert-butyl hydroperoxide (TBH) were assessed for total ROS content by flow cytometry using 2′,7′-dihydrodichlorofluorescein diacetate as described in *Section* 2. Dot Plot representation, *X* axis represents fluorescence intensity and *Y* axis forward scattering (FCS). A, wild type; B, Δ*sucA*; C, Δ*sucB*; D, Δ*lpdA*.

toxicant-exposed *E. coli* (unpublished observations). All of these findings could help the bacterium in facing oxidative stress.

Conversely to KG, succinate content decreased in tellurite-treated cells (Fig. 2B). Since KG decarboxylation occurs non enzymatically in the presence of H_2O_2 or superoxide to yield succinate and CO_2 [12], one would expect to some extent that the increased KG content observed in tellurite-exposed cells results in augmented succinate levels. Probably succinate amounts could be augmented only after enough KG is accumulated and thus succinate coming from KG decarboxylation would serve to keep the Krebs cycle at work under basal conditions.

3.3. Transcriptional level of sucA, sucB and lpdA in tellurite-exposed E. coli

To assess if the observed decrease of KGDHc activity in tellurite-treated cells was related to the amount of *sucA*, *sucB* or *lpdA* transcripts, their levels were analyzed by qPCR. Significant changes were observed only for the *sucA* gene. While *sucB* and *lpdA* transcription was not altered significantly, that of *sucA* was decreased by ~50% (Fig. S1B). Although not totally conclusive, these results possibly reveal that tellurite inhibits KGDHc activity by affecting the amount of the E1 component transcript rather that exerting a direct effect on the $[(SucA)_{12}$-$(SucB)_{24}$-$(Lpd)_2]$ multienzyme complex. Decreased *sucA* transcription would result in less SucA to form further complexes and hence in decreased enzymatic activity, which also would slow the functioning of the Krebs cycle. Decreased *E. coli sucA* transcription has also been observed in *E. coli* cells exposed to TiO_2 [21].

3.4. Tellurite susceptibility of E. coli deficient in KG metabolism

A wild type *E. coli* as well as Δ*sucA*, Δ*sucB* and Δ*lpdA* strains was analyzed to assess tellurite tolerance. All mutant derivatives showed increased tellurite sensitivity in regard to the isogenic, parental strain (Table 2). Particularly interesting was the Δ*lpdA* strain, which was eightfold more sensitive to tellurite than wild type cells. It should be noted that tellurite concentrations used in these experiments could affect, in addition to the Krebs cycle, other metabolic pathways such as glycolisis [22], the pentose phosphate shunt and/or the electron transport chain (unpublished data), which would inhibit bacterial growth.

3.5. ROS content in tellurite-exposed E. coli

Total ROS as well as superoxide content was assessed in tellurite-exposed *E. coli*. Regarding the respective untreated controls, increased levels of superoxide and total ROS were observed in all tellurite-treated cells (Figs. 3 and 4). Increased levels of these species were more evident in the wild type strain. At least 20% less

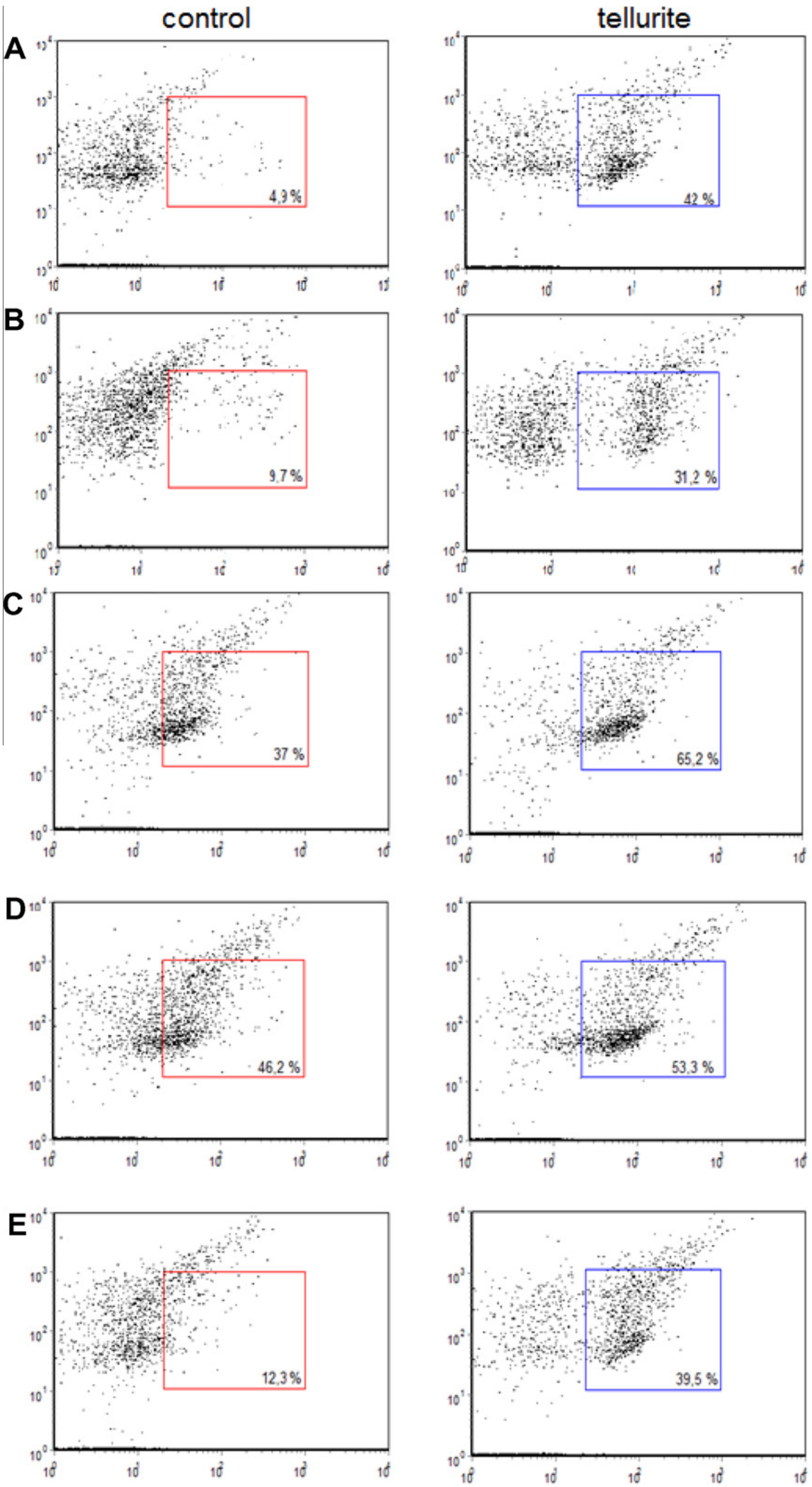

Fig. 4. Superoxide generation in tellurite-exposed *E. coli*. The indicated *E. coli* strains exposed or not to tellurite were assessed for superoxide content by flow cytometry using dihydroethidine as described in Section 2. Dot Plot representation, *X* axis represents fluorescence intensity and *Y* axis forward scattering (FCS). A, wild type; B, Δ*sodAB*; C, Δ*sucA*; D, Δ*sucB*; E, Δ*lpdA*.

total ROS was observed in tellurite-treated mutant strains as compared to the wild type counterpart. This could be interpreted as the lack of KGDHc activity in mutant strains resulting in KG accumulation which could be used in ROS scavenging.

Finally, all tested strains exhibited high basal superoxide levels. This could be explained because KGDHc inhibition/inactivation would interrupt the functioning of the Krebs cycle, which in turn would result in a decreased cellular antioxidant pool. In addition, dihydroethidine becomes very toxic after being oxidized by superoxide because of its interaction with DNA [23]. Regarding the respective controls, fluorescence intensity increased 37%, 28%, 7% and 28% in tellurite-exposed wild type, Δ*sucA*, Δ*sucB* and Δ*lpdA*, respectively. These results support those obtained when analyzing total ROS content. To shed further light to the tellurite effect on global KG metabolism, experiments regarding KG biosynthesis upon tellurite exposure are currently being carried out in our laboratory.

Acknowledgments

This work was supported in part by Grants # 1090097 from Fondecyt (Fondo Nacional de Investigación Científica y Tecnológica) and Dicyt-USACH (Dirección de Investigación en Ciencia y Tecnología-Universidad de Santiago de Chile) to C.C.V. C.A.R. was supported by a doctoral fellowship CONICYT (Comisión Nacional de Investigación Científica y Tecnológica). C.A. was supported by the Ontario Graduate Scholarship and Laurentian University.

Appendix A. Supplementary data

Supplementary data associated with this article can be found, in the online version, at http://dx.doi.org/10.1016/j.bbrc.2012.04.069.

References

[1] D. Taylor, Bacterial tellurite resistance, Trends Microbiol. 7 (1999) 111–115.

[2] S. Baesman, T. Bullen, J. Dewald, et al., Formation of tellurium nanocrystals during anaerobic growth of bacteria that use Te oxyanions as respiratory electron acceptors, Appl. Environ. Microbiol. 73 (2007) 2135–2143.

[3] F. Borsetti, V. Tremaroli, F. Michelacci, et al., Tellurite effects on *Rhodobacter capsulatus* cell viability and superoxide dismutase activity under oxidative stress conditions, Res. Microbiol. 156 (2005) 807–813.

[4] I. Calderón, F. Arenas, J.M. Pérez, et al., Catalases are NAD(P)H dependent tellurite reductases, PLoS ONE 1 (2006) e70.

[5] V. Tremaroli, F. Fedi, D. Zannoni, Evidence for a tellurite-dependent generation of reactive oxygen species and absence of a tellurite-mediated adaptive response to oxidative stress in cells of *Pseudomonas pseudoalcaligenes* KF707, Arch. Microbiol. 187 (2006) 127–135.

[6] J.M. Pérez, I.L. Calderón, F.A. Arenas, et al., Bacterial toxicity of potassium tellurite: unveiling an ancient enigma, PLoS ONE 2 (2007) e211.

[7] J. Tantaleán, M. Araya, S. Pichuantes, et al., The *Geobacillus stearothermophilus* V *iscS* gene, encoding cysteine desulfurase, confers resistance to potassium tellurite in *Escherichia coli* K-12, J. Bacteriol. 185 (2003) 5831–5837.

[8] I.L. Calderón, A.O. Elías, E.L. Fuentes, et al., Tellurite-mediated disabling of 4Fe–4S clusters of *Escherichia coli* dehydratases, Microbiology 155 (2009) 1840–1846.

[9] M.E. Castro, R. Molina, W. Díaz, et al., The dihydrolipoamide dehydrogenase of *Aeromonas caviae* ST exhibits NADH-dependent tellurite reductase activity, Biochem. Biophys. Res. Commun. 375 (2008) 91–94.

[10] A. De Kok, A.F. Hengeveld, A. Martin, et al., The pyruvate dehydrogenase multienzyme complex from Gram-negative bacteria, Biochim. Biophys. Acta 1385 (1998) 353–366.

[11] R.J. Mailloux, R. Bériault, J. Lemire, et al., The tricarboxylic acid cycle, an ancient metabolic network with a novel twist, PLoS ONE 2 (2007) e690.

[12] N.I. Fedotcheva, A.P. Sokolov, M.N. Kondrasshova, Nonenzymatic formation of succinate in mitochondria under oxidative stress, Free Radic. Biol. Med. 41 (2006) 56–64.

[13] D.E. Fuentes, E.L. Fuentes, M.E. Castro, et al., Cysteine metabolism-related genes and bacterial resistance to potassium tellurite, J. Bacteriol. 189 (2007) 8953–8960.

[14] M. Bradford, A rapid and sensitive method for quantitation of microgram quantities of protein utilizing the principle of protein-dye-binding, Anal. Biochem. 72 (1967) 248–254.

[15] G.A. Pradenas, B.A. Paillavil, S. Reyes-Cerpa, et al., Reduction of the monounsaturated fatty acid content of *Escherichia coli* K-12 results in increased resistance to oxidative damage, Microbiology 158 (2012) 1279–1283.

[16] R. Hamel, V. Appanna, Modulation of TCA cycle enzymes and aluminum stress in *Pseudomonas fluorescens*, J Inorg. Biochem. 87 (2001) 1–8.

[17] R. Singh, D. Chénier, R. Bériault, et al., Blue native polyacrylamide gel electrophoresis and the monitoring of malate- and oxaloacetate-producing enzymes, J. Biochem. Biophys. Methods 64 (2005) 189–199.

[18] R. Mailloux, R Singh, G. Brewer, et al., α-ketoglutarate dehydrogenase and glutamate dehydrogenase work in tandem to modulate the anti-oxidant α-ketoglutarate during oxidative stress in *Pseudomonas fluorescens*, J. Bacteriol. 191 (2009) 3804–3810.

[19] J. Middaugh, R. Hamel, G. Jean-Baptiste, et al., Aluminum triggers decreased aconitase activity via Fe–S cluster disruption and the overexpression of isocitrate dehydrogenase and isocitrate lyase: a metabolic network mediating cellular survival, J. Biol. Chem. 280 (2005) 3159–3165.

[20] R. Singh, R. Mailloux, S. Puiseux-Dao, V.D. Appanna, Oxidative stress evokes a metabolic adaptation that favors increased NADPH synthesis and decreased NADH production in *Pseudomonas fluorescens*, J. Bacteriol. 189 (2007) 6665–6675.

[21] Y. Ojima, M. Nishioka, M. Taya, Metabolic alternations in SOD-deficient *Escherichia coli* cells when cultivated under oxidative stress from photoexcited titanium dioxide, Biotechnol. Lett. 30 (2008) 1107–1113.

[22] M.A. Valdivia, J.M. Pérez-Donoso, C.C. Vásquez, Effect of tellurite-mediated oxidative stress on the *Escherichia coli* glycolytic pathway, Biometals 25 (2012) 451–458.

[23] C.D. Georgiou, I. Papapostolou, N. Patsoukis, T. Tsegenidis, T. Sideris, An ultrasensitive fluorescent assay for the in vivo quantification of superoxide radical in organisms, Anal. Biochem. 347 (2005) 144–151.

[24] T. Baba, T. Ara, M. Hasegawa, et al., Construction of *Escherichia coli* K-12 in-frame, single-gene knockout mutants: the Keio collection. Mol. Syst. Biol. 2 (2006) 2006.0008.